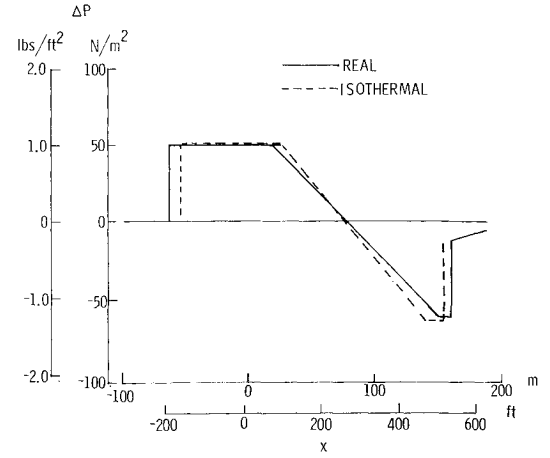

Fig. 2 Signatures resulting from real and isothermal atmospheres.

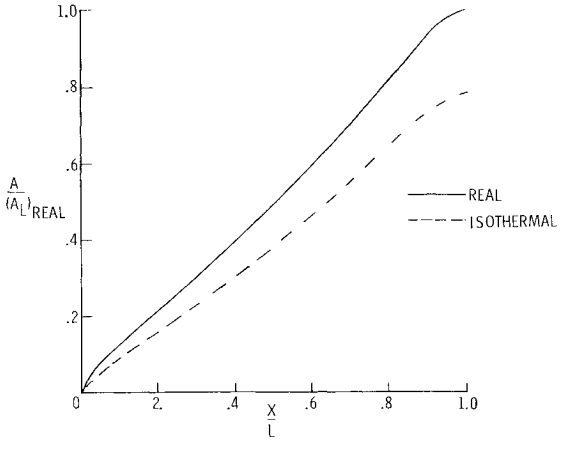

Fig. 3 Normalized area distributions. $A_{L,REAL} = 976.263$ ft^2 (90.697m^2).

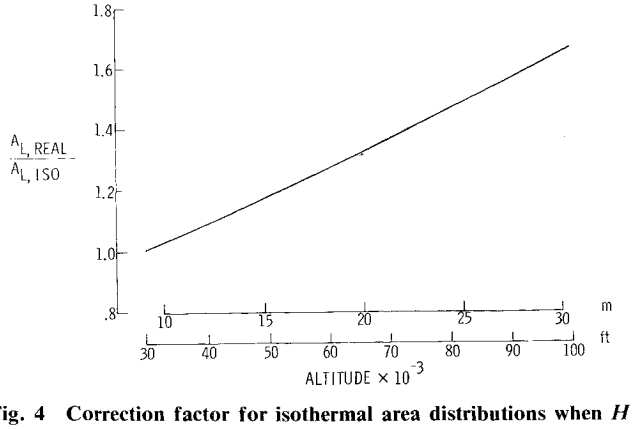

Fig. 4 Correction factor for isothermal area distributions when H = 25,000 ft.

equivalent area, A_L, at the equivalent length, L, is proportional to W/q, where W is the cruise weight and q, the dynamic pressure. At constant Mach number and with a pressure scale height of 25,000 ft, the isothermal approximation for q yields equivalent area distributions that are too low to reflect the cruise weight requirements at the given altitude and Mach number in the real atmosphere (Fig. 3). Within the isothermal approximation, A_L may be corrected in one of two ways: using the correct value for q at the given altitude or selecting the scale height which gives the proper pressure at altitude. For the given conditions at $M = 3$, the correct q yields the correct area distribution to within 3% but Δp was overpredicted by 20%. Alternatively, changing the scale height corrects the area distribution to within 1.5% of

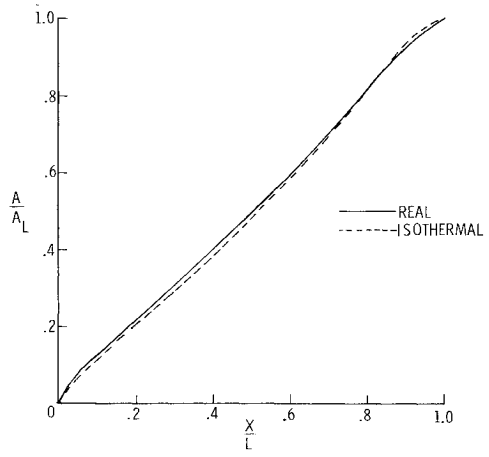

Fig. 5 Comparison of normalized area distributions.

the real distribution but overpredicts Δp by 8%. Thus, it appears that the most accurate prediction of Δp occurs when using a scale height of 25,000 ft in the isothermal atmosphere. The resulting area distribution may be improved by the factor $A_{L,Real}/A_{L,ISO}$. For a scale height of 25,000 ft, values of this ratio as a function of altitude are shown in Fig. 4. After correction, the isothermal distribution differs by less than 8% from the real atmosphere distribution (Fig. 5). This corrected area distribution overpredicts Δp by 5% after propogation through the real atmosphere.

Thus, for sonic boom minimization studies in mid-range supersonic Mach numbers, use of the isothermal atmosphere with a scale height of 25,000 ft provides reliable estimates of overpressures, and a simple adjustment to the isothermal equivalent areas provides a good approximation to the correct area distribution. However, for design studies, propagation of a known F function or minimization studies at low supersonic Mach numbers, the isothermal approximation to the real atmosphere becomes unsatisfactory.

References

[1] Seebass, A.R. and George, A.R., "Sonic Boom Minimization," *Journal of the Acoustical Society of America*, Vol. 51, Feb. 1972, pp. 686-694.

[2] Seebass, A. R. and George, A. R., "Design and Operation of Aircraft to Minimize their Sonic Boom," *Journal of Aircraft*, Vol. 11, Sept. 1974, pp. 509-517.

[3] George, A. R. and Plotkin, K. J., "Sonic Boom Waveforms and Amptitudes in a Real Atmosphere," *AIAA Journal*, Vol. 7, Oct. 1969, pp. 1978-1981.

[4] Warren, C. H. E., "A Significant Single Quantity that Typifies a Sonic Bang," *Journal of the Acoustical Society of America*, Vol. 51, Jan. 1972, pp. 418-420.

Static Stability and Aperiodic Divergence

Gottfried Sachs*
Techniche Hochschule Darmstadt, Darmstadt, W. Germany

Nomenclature

B,C,D,E	= coefficients of the characteristic equation
g	= acceleration due to gravity
I_y	= pitch moment of inertia

Received October 21, 1974. The author wishes to acknowledge the help of Professor Dr.-Ing. X. Hafer, head of the Institut für Flugtechnik.

Index category: Aircraft Handling, Stability and Control.

*Dozent, Institut für Flugtechnik.

m = mass of airplane
M_i = $(1/I_y)\partial M/\partial i$ where $i=q,\ u,\ \alpha,\ \dot{\alpha}$, pitching moment derivative, including the effects of engine thrust
q = angular velocity in pitch
R = Routh's discriminant
$1/T_{div}$ = unstable root
u = pertubation of speed (longitudinal)
U_o = trim speed
w = pertubation of speed (vertical)
X_i = $(1/m)\partial X/\partial i$ where $i=u,\ w,\ \alpha$, longitudinal force derivative, including the effects of engine thrust
Z_i = $(1/m)\partial Z/\partial i$ where $i=u,\ w,\ \alpha$, vertical force derivative, including the effects of engine thrust
α = angle of attack
σ = real part of a complex variable
ω = imaginary part of a complex variable

Introduction

IT is well known that static stability is only a necessary condition for dynamic stability of longitudinal flight. In common cases, however, it is considered sufficient to prevent aperiodic divergence.[1-4] It is not known to what extent this assumption is valid and which conditions exist where static stability cannot prevent aperiodic divergence. The purpose of this Note is to show these conditions and, as a more general aspect, the cases where static stability is sufficient for dynamic stability and where it is not. The relation of static stability and aperiodic divergence is of particular interest in regard to the static stability requirement of MIL-F-8785B,[5] since this requirement banning aperiodic divergences is considered satisfied if the airplane is statically stable.

In general, the critical stability conditions[6] of the stability quartic for longitudinal flight are given by Routh's discriminant

$$R=BCD-D^2-B^2E=0 \tag{1}$$

and by the static stability boundary $E=0$, from which the latter may be expressed as

$$Z_uM_\alpha-Z_wM_u=0 \tag{2}$$

Because

$$R|_{E=0}=D(BC-D)|_{E=0}=0 \tag{3}$$

these have two points of intersection when varying M_α and M_u as the decisive factors with regard to static stability (as illustrated in the upper part of Fig. 1). They are given by

$$M_{\alpha_1}\approx Z_wM_q \tag{4}$$

and

$$M_{\alpha_2}=Z_wM_q\left[1-\frac{g(1+M_{\dot{\alpha}}/M_q)}{Z_\alpha X_u/Z_u-(X_\alpha-g)}\right] \tag{5}$$

The point denoted by M_{α_1}, which represents the maneuver point, is independent of the lift and drag characteristics. The point denoted by M_{α_2}, however, significantly changes its value with the lift and drag coefficient, as expressed by X_u, Z_u, and X_α. This can be characterized by the different conditions existing for the "front—" and "backside" of the power-required curve (when neglecting the elevator contributions X_{δ_e} and Z_{δ_e}). For "frontside" operation, i.e., for

$$X_u-(X_\alpha-g)Z_u/Z_\alpha<0 \tag{6a}$$

M_{α_2} is always positive and larger than M_{α_1}(Fig. 1). From this and the possible locations of the stability boundaries in the $M_\alpha-M_u$ plane, it follows that static stability is a sufficient condition to prevent aperiodic divergences. (For M_u values smaller than those determined by $R=0$, it is even sufficient to prevent unstable oscillations.) This is valid for $M_\alpha<M_{\alpha_1}$ or, in other words, for positive maneuver margins, thus including $M_\alpha<0$ as the center-of-gravity range of predominant importance. The case described is illustrated in Fig. 1 where the

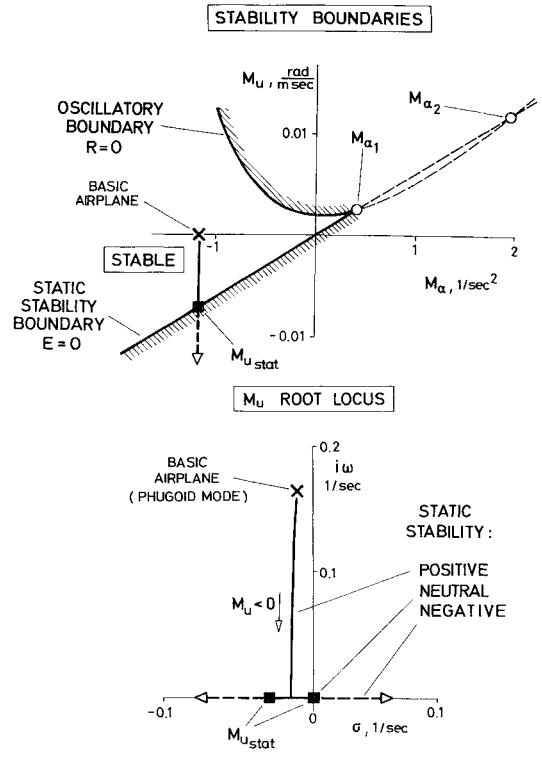

Fig. 1 Relation of static and dynamic stability for operation on the "frontside" of the power-required curve.

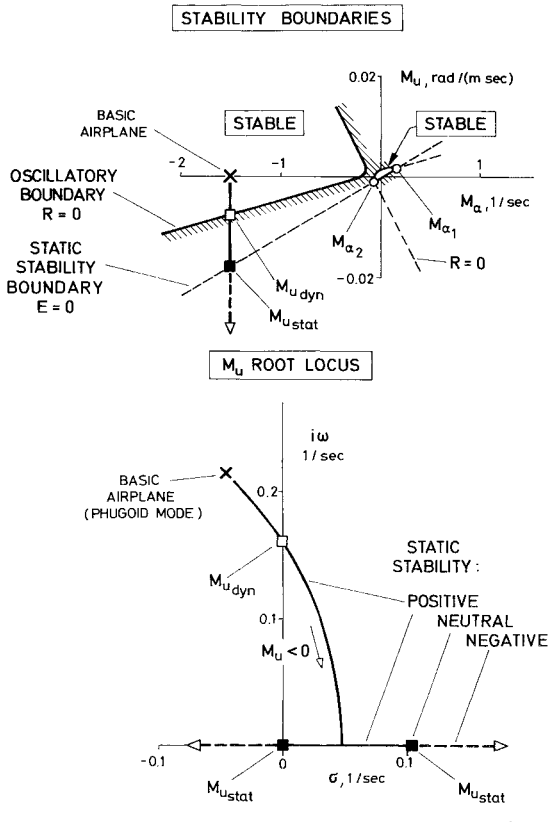

Fig. 2 Relation of static and dynamic stability for operation on the "backside" of the power-required curve.

effect of the static margin varied by M_u on the stability characteristics of a subsonic jet transport in low-speed flight is shown. The M_u values used as gains in the M_u root locus are indicated in the stability region plotted in the upper half of the figure. (Here and in the figures following, only the phugoid as the more interesting mode of motion is shown.) The relation of static and dynamic stability has altered when operating on the "backside" of the power-required curve, i.e., when

$$X_u - (X_\alpha - g)Z_u/Z_\alpha > 0 \tag{6b}$$

Because $M_{\alpha 2}$ is less than $M_{\alpha 1}$ in this case (Fig. 2), static stability is sufficient to prevent aperiodic divergences only if

$$M_{\alpha 2} < M_\alpha < M_{\alpha 1}$$

For larger angle-of-attack stability ($M_\alpha < M_{\alpha 2}$), a reduction of the static margin due to M_u leads to aperiodic divergences before static stability becomes neutral. This result follows from an investigation of the possible locations of the stability boundaries in the $M_\alpha - M_u$ plane, when combined with a root locus analysis where M_u is treated as gain. It is illustrated in Fig. 2 using a slender wing aircraft in low-speed flight as an example. As can be seen, a reduction of the static margin due to M_u initially introduces an unstable (phugoid) oscillation, with the oscillatory stability boundary $R=0$ given by

$$M_{u_{dyn}} \approx M_{u_{stat}} + \frac{(M_\alpha - M_{\alpha 2})(X_u - (X_\alpha - g)Z_u/Z_\alpha)}{X_\alpha - g + gZ_w(M_q + M_{\dot\alpha} + Z_w)/(Z_w M_q - M_\alpha)} \tag{7}$$

Here, $M_{u_{stat}}$ denotes the static stability boundary, as described by Eq. (2). This is followed by an aperiodic divergence, with the static margin still positive. When static stability is neutral, the unstable root can be approximated by

$$1/T_{div} \approx (M_{\alpha 2} - M_\alpha)\frac{X_u - (X_\alpha - g)Z_u/Z_\alpha}{Z_w M_q - M_\alpha} \tag{8}$$

It may be of interest to note that $M_{\alpha 2} > 0$ if

$$Z_\alpha X_u/Z_u - X_\alpha > g\, M_{\dot\alpha}/M_q \tag{9a}$$

Thus, the properties just described apply in the whole range of positive angle-of-attack stability ($M_\alpha < 0$). The results derived can also be used in the case $M_u = 0$ where static stability depends on M_α alone. In this case, Eq. (9a) provides the criterion whether or not static stability is a sufficient condition to prevent aperiodic divergences.

Considering first the opposite of Eq. (9a)

$$Z_\alpha X_u/Z_u - X_\alpha < g M_{\dot\alpha}/M_q \tag{9b}$$

it follows from the corresponding M_u cases described before that there are two possibilities in regard to the intersections of the oscillatory boundary $R=0$ and the M_α axis. First, no intersection exists (as shown, for example, in Fig. 1). This means that static stability, when determined by M_α alone, is a sufficient condition for dynamic stability. It requires that the following approximate expression is true (excluding STOL-flight with very large values of X_u and X_α):

$$\frac{X_u}{Z_u} > -\frac{(M_q(X_\alpha - g) - g\,Z_w)^2}{4g\,Z_\tau M_q(M_q + M_{\dot\alpha} + Z_w)} \tag{10}$$

It may be of interest to note that this does not necessarily imply operation on the "frontside" of the power-required curve only. It may also be true for "backside" operation. The second possibility is that the two intersections of the oscillatory boundary $R=0$ and the M_α axis exist. This is shown in the upper part of Fig. 3, with the intersections

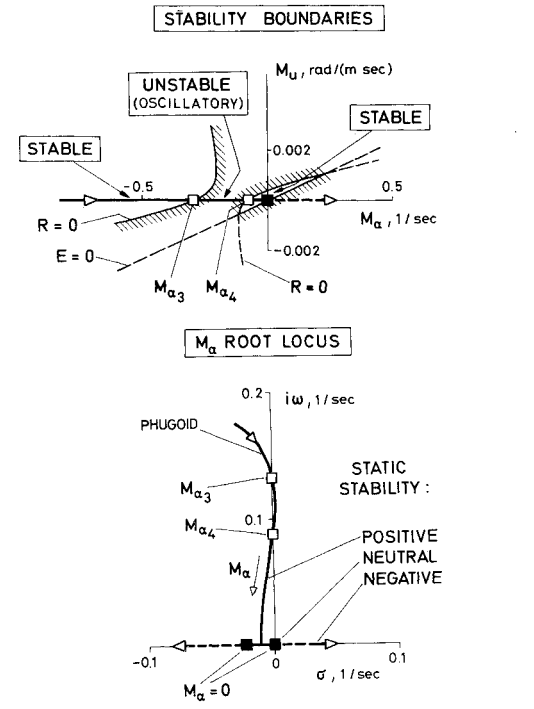

Fig. 3 Static stability preventing aperiodic divergence, M_α effect only.

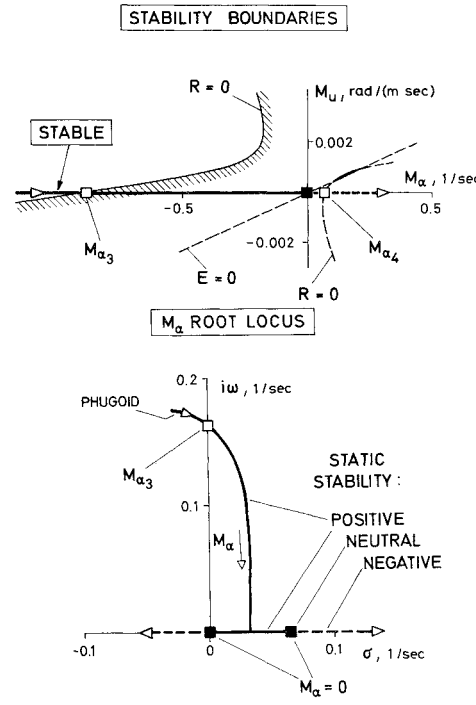

Fig. 4 Static stability not preventing aperiodic divergence, M_α effect only.

denoted by $M_{\alpha 3}$ and $M_{\alpha 4}$. The M_α range enclosed by $M_{\alpha 3}$ and $M_{\alpha 4}$ is dynamically unstable. The range between $M_{\alpha 4}$ and the origin ($M_\alpha = 0$), however, is stable, provided that the intersections $M_{\alpha 3}$ and $M_{\alpha 4}$ both are located on the left hand side of the origin. This is the case, if Eq. (9b) is true. As a result, there is always a certain range of dynamically stable M_α values adjacent to the origin (as the point of neutral static stability). From this and a corresponding root locus analysis, it follows that static stability is a sufficient condition to prevent aperiodic divergences in the case under consideration. This is illustrated in Fig. 3, where the effect of the static margin varied by M_α on the stability characteristics of a

supersonic transport in low-speed flight is shown. As can be seen in this example, there is dynamic instability in the statically stable M_α range enclosed by $M_{\alpha 3}$ and $M_{\alpha 4}$. From the root loci possible, it follows that this can only be an unstable oscillation and not a divergence.

In the second case of interest, the opposite of Eq. (9b) has to be considered. The corresponding M_u case has shown that $M_{\alpha 2}>0$. From this and the possible location of the stability boundaries it follows, that the origin $M_\alpha=0$ now lies between the intersections $M_{\alpha 3}$ and $M_{\alpha 4}$. This means that it lies in an unstable region. As a result, a reduction of M_α now leads to an aperiodic divergence before the static stability boundary is approached. This is illustrated in Fig. 4, which shows the characteristics of the SST of Fig. 3 when the drag-due-to-lift slope $\partial C_D/\partial C_L$ is assumed to be doubled. The instability developing is such that a reduction of M_α initially introduces an unstable oscillation. This is the case when M_α approaches the value

$$M_{\alpha 3} \approx 2\, Z_w M_q + (Z_u/X_u)(g\, Z_w - (X_\alpha - g)M_q)/U_o \qquad (11)$$

A further reduction of the static margin, being still positive, converts the unstable oscillation into a divergence. Its unstable root at the static stability boundary can be approximated by

$$1/T_{div} \approx X_u - (Z_u/Z_\alpha)\ (X_\alpha + g\, M_{\dot\alpha}/M_q) \qquad (12)$$

References

[1] Chalk, C.R., Neal, T.P., Harris, T.M., Pritchard, F.E., and Woodcock, R.J., " Background Information and User Guide for MIL-F-8785B(ASG), Military Specification-Flying Qualities of Piloted Airplanes," AFFDL-TR-69-72, August 1969, Air Force Flight Dynamics Lab., Wright-Patterson Air Force Base, Ohio.

[2] Chalk, C.R., Key, D.L., Kroll, J. Jr., Wasserman, R., and Radford, R.C., "Background Information and User Guide for MIL-F-83300-Military Specification—Flying Qualities of Piloted V/STOL Aircraft," AFFDL-TR-70-88, March 1971, Air Force Flight Dynamics Lab., Wright-Patterson Air Force Base, Ohio.

[3] Hacker, T., Hacker, T., *Flight Stability and Control,* American Elsevier Publishing Co., New York, 1970.

[4] Babister, A.W., *Aircraft Stability and Control,* Pergamon Press, Oxford, 1961.

[5] *Military Specification—Flying Qualities of Piloted Airplanes,* MIL-F-8785B(ASG), August 1969.

[6] Etkin, B., *Dynamics of Atmospheric Flight,* Wiley, New York, 1972.

Errata

Design of Crashworthy Aircraft Cabins Based on Dynamic Buckling

C.A.Fisher and C.W.Bert
University of Oklahoma, Norman, Okla.

[J. Aircraft **10**, 693-695 (1973)]

THE quantities J_r and J_s represent the torsional rigidity constants of the rings and stringers, respectively, and not the polar moments of inertia. This changes the corresponding colums in Table 1 to read as follows:

Aircraft	J_{s_4} (in.)	J_{r_4} (in.)
A	0.000005	0.000027
B	0.00016	0.000057
C	0.00001	0.00014
D	0.000006	0.000049
Representative	0.00001	0.00014

Table 2 Buckling analysis results

Subshell	$\bar F_{cr}$	n at $\bar F_{cr}$
I	1.21	17
II	1.76	17
III	2.20	17

Table 3 Influence of number of stringers on buckling load of SSII

Number of stringers, M	$\bar F_{cr}$
30	1.02
40	1.16
50	1.27
60	1.38

Received November 11, 1974.
Index categories: General Aviation Systems; Structural Dynamic Analysis; Aircraft Structural Design (Including Loads).

Table 4 Influence of spacing on buckling load

Dimensionless ring spacing, l/R	$\bar F_{cr}$
0.50	1.96
0.75	1.68
1.00	1.52
2.00	1.21

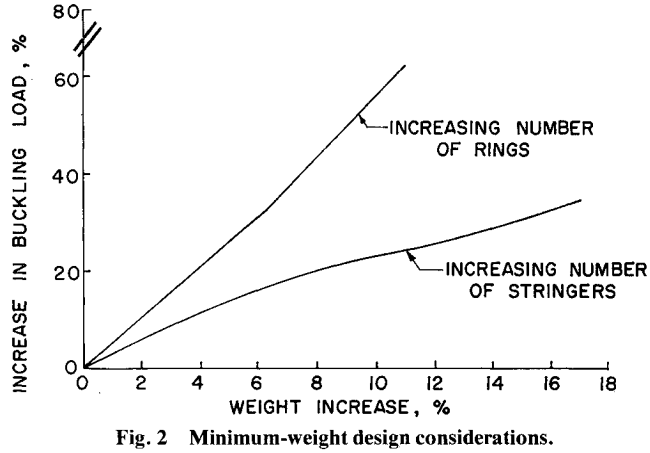

Fig. 2 Minimum-weight design considerations.

The above changes in input data for the representative aircraft changed Tables 2, 3 and 4 and Fig. 2 as will be shown. It is noted that reducing J_s and J_r by two and three orders of magnitude respectively reduces the dimensionless buckling load $\bar F_{cr}$ by as much as about 57%. However, the qualitative trends are the same as before and the number of circumferential waves at buckling were increased from 15 to only 17.

In the first paragraph of the section on "Modeling Using Subshells" (p. 694), reference was inadvertently made to Table 1 instead of Table 2.

The authors would like to thank J. Singer, Department of Aeronautical Engineering, Technion—Israel Institute of Technology, Haifa, Israel for bringing the discrepancies in J_r and J_s to their attention. The computational assistance of T. Chen, graduate student, and use of the IBM 370 computer at the Merrick Computing Center of the University of Oklahoma are also acknowledged.